参赛队员姓名：程天葭，洪昀伦

中学：上海中学国际部

省份：上海

国家/地区：中国

指导教师姓名：刘佳龙，曹宵鸣

指导教师单位：上海中学国际部，华东理工大学

论文题目：O_2 Activation on MN_4 Embedded Nanotube Catalyst (M = 3d Transition Metal)

O_2 Activation on MN_4 Embedded Nanotube Catalyst (M = 3d Transition Metal)

Authors: 程天葭, 洪昀伦

Abstract

Methane (CH4) as a source of fuel possesses high economic efficiency in terms of energy density and abundance. For the effective usage of methane, the conversion of gaseous methane into liquid fuels (such as methanol) with catalysts is required. Porphyrin-like structures featuring MN_4 have been shown to have promising effects on the oxygen reduction reactions that are used in the conversion of methane. Using density functional theory (DFT) calculations, this study tries to evaluate and compare both the effects of nanotube radius and transition metal center on the adsorption of oxygen and activation energies of the MN co-doped system. After analysis the results show that the adsorption energies of the various sizes of nanotube to be more negative than flat graphene surfaces, and is shown to be able to effectively reduce the energy barrier and increase the likeliness of methane hydrocarbon bond activation reactions. Through the analysis of absorption energy, Bader charge and oxygen species of various nanotubes with different period 3 transition metals, it is discovered that oxygen absorption is weaker among transition metals on the rightward side of the periodic table. This work provides further insights to the different methods in finding the most efficient MN_4 embedded nanotube catalysts.

Keywords: nanotube, oxygen activation, porphyrin, catalysis

Table of Contents:

1. Introduction

Natural gases (mainly methane), possesses superior economic efficiency in comparison to other fossil fuels, with its high energy density (>1000 kWh/m^3) and abundance, but due to methane's gaseous state, it is often hard to be transported and thus used[1-2]. The development of efficient methods for the conversion of methane into liquid fuels have become increasingly important for the usage of cheap natural gases. Conventional two-step methods of converting methane to methanol offers a stable solution to methane transportation, but is often cost- and energy-ineffective due to the high bond enthalpy of C-H[3-4].

On the other hand, the usage of oxygen reduction reactions (ORR) has offered an alternative pathway to methane activation with lower energy barriers. This allows for a more efficient and less costly route to methane activation. However, current methods to catalyze the reaction often involves in equally expensive metals such as palladium[5].

In the context of new biology-inspired catalysts, porphyrin-like structures of MN_4 have been shown to have promising effects on oxygen reduction reactions. Porphyrin structures are found naturally in biosystems in relation to O2 delivery and storage[6]. And metal doped graphene have been confirmed that they exhibit catalytic behaviors as due to graphene's excellent electrical and thermodynamic properties[7-8]. The incorporation of MN4 structures onto graphene and carbon nanotubes (CNTs) have been demonstrated to have improved catalytic performance [9-11].

The electron configuration of the metal center of the MN4 site is shown to influence the activity and stability of the active site [12,13]. Therefore, changing different M centers could also pose an effect on the efficiency and energy requirements of the reaction. In this experiment, different 3d transition metals are used to better understand the effects of electron configuration on catalytic effect.

The ORR activity and stability are also highly influenced by the carrier that carries it. It is also shown that, when using CNTs, the catalytic effect is also highly related to its tube diameter and length, due to their influence on the geometrical and electronic structure of the CNTs. Little systematic research is reported to investigate the influence and cause of the change in catalytic ability. Thus, in this study nanotubes of different radii are investigated by their effects on oxygen's catalytic abilities[14].

This study applies the density functional theory (DFT) method to computationally evaluate the influence of tube diameter and M center to the catalytic effects of MN4 structures

embedded on CNTs. DFT is chosen due to its ability to enable analysis in atomic levels, which is needed to compare the different effectiveness of the metals and tube size.

2. Methodology

All calculations were carried out using the Vienna Ab-initio Simulation Package (VASP) with the projector augmented wave method and a cutoff energy of 500eV[15-17]. The generalized gradient approximation method was chosen with Perdew-Burke-Ernzerhof (PBE) functional for the exchange-correlation term [18].

Adsorption geometries underwent optimization using a force-based gradient algorithm until forces for all atoms were below 0.05 eV/Å. The transition states (TSs) of methane activation were searched with a constrained optimization scheme[19]. The optimized state was when the total energy was a maximum in the reaction coordinate, and minimum compared to the degrees of freedom.

A periodic slab model was used to simulate the MN_4-nanotube catalyst with cells of varying sizes depending on the dimensions of the nanotubes. The specifics of the dimensions would be specified in the following sections. To reduce the amount of required computing power for optimizing nanotubes of increasing sizes and number of atoms, the team has decided to cleave the nanotubes used in the investigation of effects of radius on catalytic ability in the following manner:

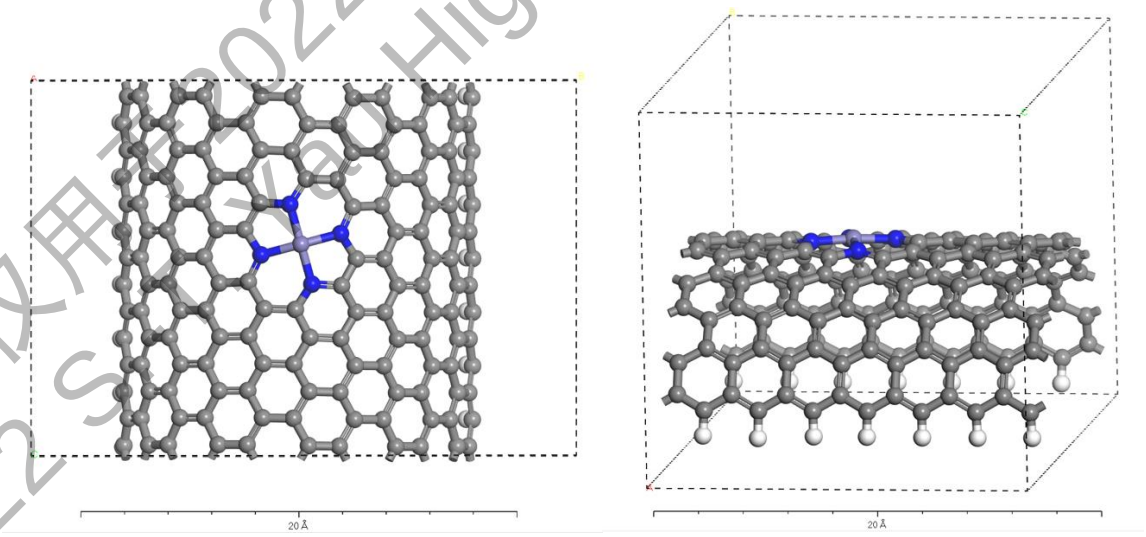

Figure 1. Top and Side Views of Cleavage

Each nanotube will be cleaved until four rows of carbon remain on each side. The ring structure of the rows are preserved, and the last bond of the carbon at the cut site is replaced with a C-H bond, with the hydrogen fixed during optimizations. For trials made to experiment with transition metals and their effectiveness as catalysts, a 25Å*25Å*17.2159Å full-sized cell was used. The specific cell size for each dimension is stated in appendix.

2.1 Density of States (DOS) Analysis

Density of states (DOS) refers to the energy levels of electrons in a crystal, the calculation of which can be used to deduct the specific electron transfer from each orbital of an atom. Through the analysis of DOS, the specific process of electron transfer in a reaction can be deducted[20].

2.2 Nanotube Radii Determination

In the investigation of the effects of nanotube radius on the catalytic abilities of oxygen, the dimensions of the nanotubes are adjusted. Single walled nanotubes can be defined as graphene rolled into a tube of radius R in helicities that are defined by the chiral indices (n,m) where both n and m are integers. Therefore, chiral indices specify the perimeter vector or chiral vector, which in turn would determine the diameter and helictity of the nanotube.

The chiral indices determine the type of nanotube, namely when the indices are equal to (n,0), it is defined as a zigzag nanotube, one with (n,n) or n=m would be an armchair nanotube, and (n,m) equals to chiral nanotubes. As different types exhibit different properties, the type of nanotube is controlled to armchair only[21]. Thus the numbers used to represent each size equals to the n and m vectors instead of the radius in angstroms.

2.3 Embedded Energy Calculation

For the manufacturing of the poryphyrin-like co-doped nanotubes, the embedded energy required in the insertion of transition metals are calculated as follows:

$$E_{embedded} = E_M^* - (E_{sur} + E_M)$$

$E_{embedded}$ represents the embedded energy, E_M^* represents the total energy of the surface after the metal is embedded, E_{sur} represents the total energy of the N_4-doped surface, and E_M is the energy

of the chosen metal in gaseous state. A negative $E_{embedded}$ represents that energy is released in the process of embedding the metal.

2.4 Adsorption Energy Calculation

According to Sabatier's principle, the catalytic performance of the catalyst is correlated to the adsorption energy of the adsorbate at the active site. Thus, to find the most favorable adsorption configuration with the highest catalytic performance, the adsorption energies of the poryphrin-like co-doped nanotubes of different dimensions were investigated, using the formula below:

$$E_{ads} = E_x^* - (E_x + E_M^*)$$

E_x^* represents the total energy of the surface after the adsorption of oxygen, E_M^* represents the total energy of the MN_4 doped nanotube surface, and E_x represents the energy of the gaseous O_2 molecule.

The adsorption of O_2 over the central transition metal (Fe) on various-sized nanotubes through bonding O_2's bond with metal's 2pi orbitals are compared.

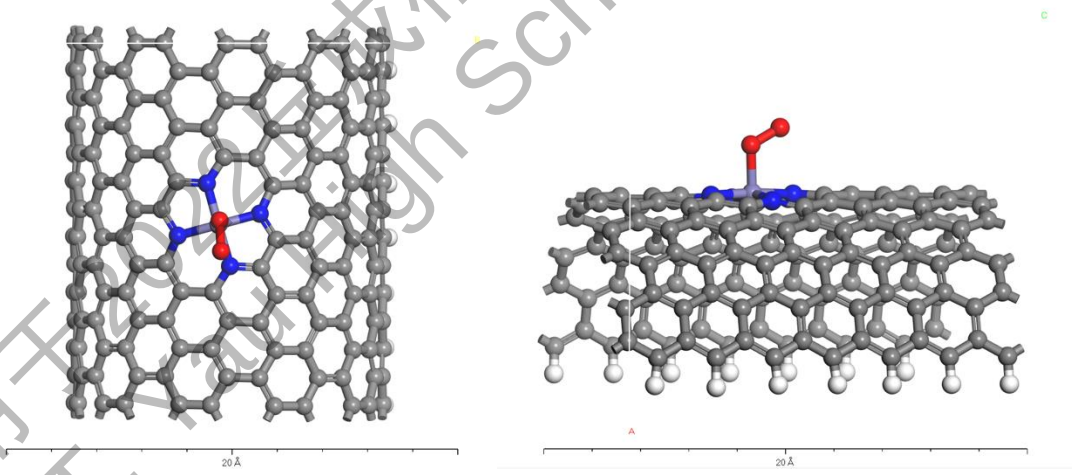

Figure 2. Top and Side Views of the Adsorption of O_2 on FeN_4-Nanotube Structure

2.5 Bader Charge Calculation

Bader charge refers to the electrons retained in an atom, where an atom is defined as division from molecules by zero flux surface. Bader charge can be used to determine the change in charge of atoms after reactions[22].

2.6. Energy Barrier Calculation

As proven by previous research, the adsorption strength of O_2 is higher than CH_4, meaning that when the two reactants are exposed to the nanotube system, O_2 is more likely to occupy the active site of the single metal atom[23]. After the adsorption of O_2, the oxidative methane activation begins.

The Eley-Rideal mechanism is proposed by previous researches as the first steps of such oxidation reactions, where the CH_4 interacts with the activated O_2 on the surface (demonstrated in *Figure 3*) in the transition states[24]. For the calculation of energy barriers of methane oxidative dehydrogenation on the surface, the energy of the structure in transition state is first found. The calculation is as follows:

$$\text{Energy Barrier} = E_{transition} - (E_M * + E_M + E_{CH4})$$

where the $E_{transition}$ is the total energy of the nanotube surface in transition state, E_M* is the energy of the total energy of the MN_4 doped surface, and E_{CH4} is the energy of methane in gaseous state.

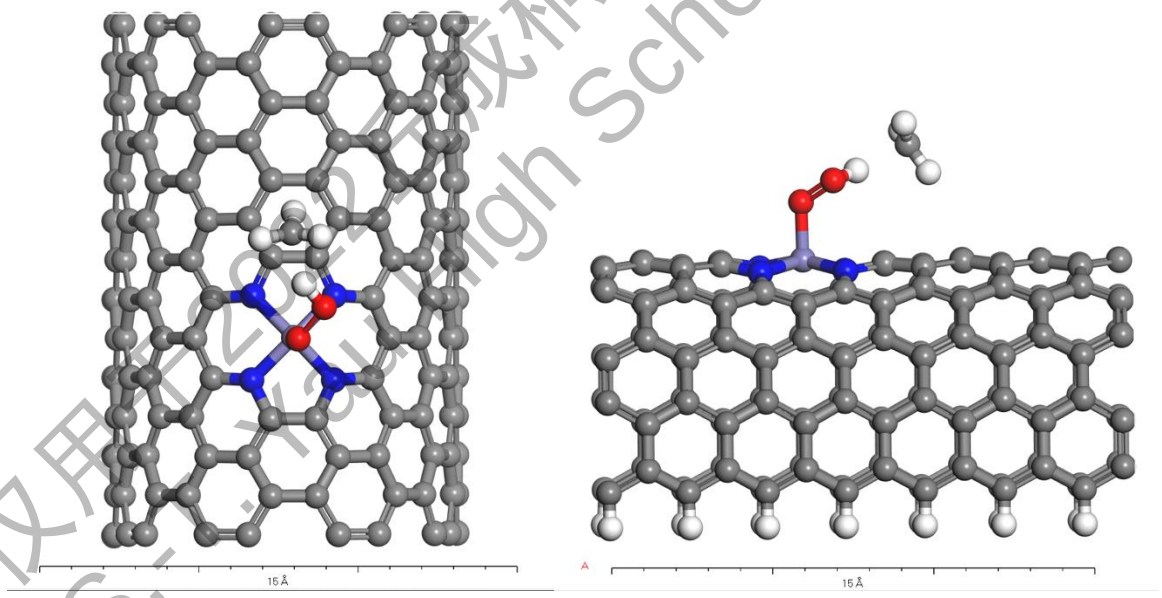

Figure 3. Top and Side Views of the Modeled Transition State of Methane Oxidative Dehydrogenation on FeN4 Doped Nanotube Surface

3. Results

3.1 Effect of Transition Metal Type on Nanotube

3.1.1 Effect of Transition Metal Type on Embedded Energy

Through the use of VASP, embedded energy is calculated, aiding to determine the difficulty of industrial synthesis, as shown in *Figure 4*. Embedded energy of all metals are negative, thus are all thermodynamically favorable.

The more negative the embedded energy is, the stronger is the interaction between the metal atom and empty nanotube surface. The embedded energy gradually approaches positive values, indicating a decrease in energy released from the embedding of metals into nanotube, thus the attraction between metal and nanotube surface decreases. This trend can be explained by atomic radii. From the left to right of the periodic table, transition metals have decreasing atomic radii, thus the distance between metal atoms and surrounding nitrogen atoms in nanotube surface gradually increase. According to Coulomb's Law, increased distance means decreased attraction force. Therefore, transition metal atomic radius gradually increases, thus attraction force between transition metal and nanotube decreases, leading to the trend of gradually approaching positive values.

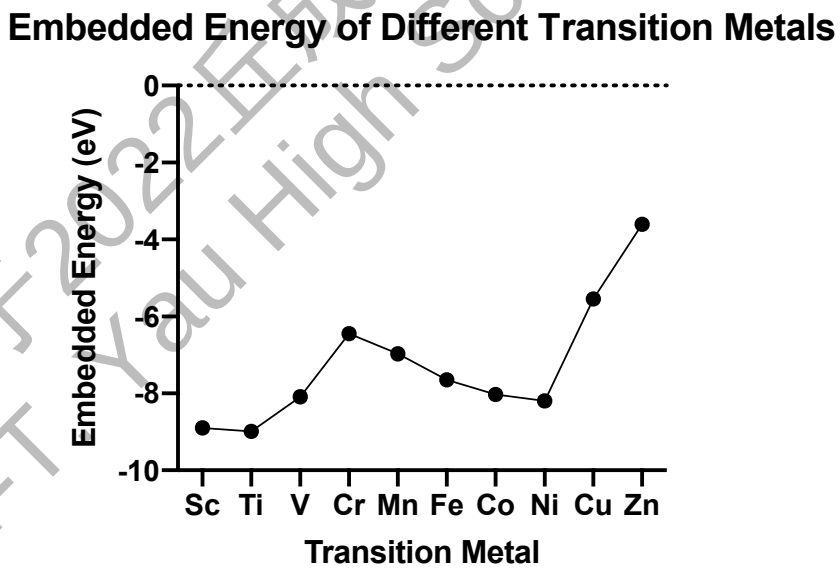

Figure 4. Embedded Energy of Different Transition Metals

3.1.2 Effect of Transition Metal Type on Oxygen Activation

3.1.2.1 Adsorption Energy of Oxygen Activation

Through the use of VASP, adsorption energy is calculated, aiding evaluation of prospect in synthesized industrially for catalysis, as shown in *Figure 5*. The more negative the adsorption energy, the stronger is the interaction between oxygen and metal-embedded nanotube. Adsorption energy displays a gradual approach to positive values, indicating a decrease in energy released from the adsorption of oxygen to metal-embedded nanotube, thus the adsorption of oxygen becomes weaker.

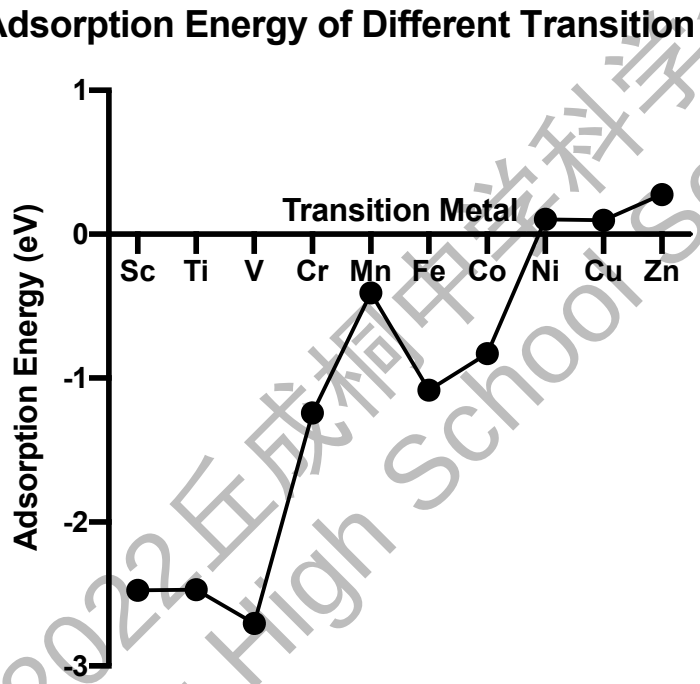

Figure 5. Adsorption Energy of Different Transition Metals

3.1.2.2 Bader Charge of Oxygen Activation

To further explore the underlying mechanism of trends exhibited in adsorption energy, bader charge is calculated through VASP, tracking the charge transfer from metal atom to the bonded oxygen atom. The more negative the bader charge, the more electrons are transferred from metal atom to oxygen. As seen in *Figure 6*, bader charge gradually approaches to positive values, indicating a decrease in electron transfer from metal atom to oxygen. This trend is correspondant to that of adsorption energy, where rightward transition metals display weaker oxygen adsorption. Therefore, it can be deducted that rightward transition metals transfer less

electrons to oxygen, thus bonds formed are weaker, adsorption energy are higher and that oxygen adsorption is weaker.

Figure 6. Bader Charge of Oxygen Atom After Oxygen Adsorption

3.1.2.3 Oxygen Species and Spin Charge of Oxygen Activation

To evaluate the conditions of oxygen adsorption, spin charge and O-O bond length are calculated to determine the oxygen species. Based on the O-O bond length, < 1.28Å is oxygen, 1.28Å-1.4Å is peroxide, > 1.4Å is superoxide. As shown in *Figure 7*, almost all oxygen species are peroxide, besides Ni and Cu being oxygen. In general, the O-O bond length displays a decreasing trend from left to right. The longer the O-O bond, the greater the influence metal atoms have on oxygen. Therefore, it is displayed that the extent of influence of most metals on oxygen remain similar, yet the influence gradually becomes weaker. This can be explained as d-orbitals become more saturated for rightward metals, thus they are less likely to lose electrons to attract oxygens, resulting in reducing influences.

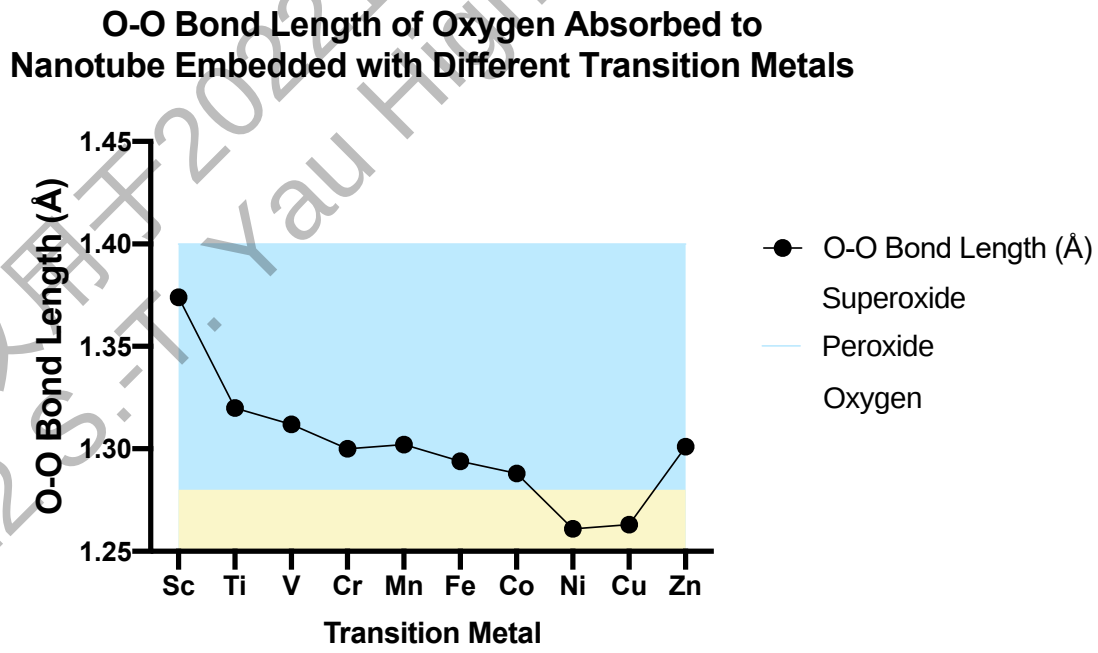

Figure 7. O-O Bond Length of Oxygen Activated MN_4 Nanotube

3.1.2.4 Discussion of Special Points

3.1.2.4.1 Ni, Cu and Zn

Ni and Cu display a significantly more positive bader charge than the other transition metals, showing adsorption energy of positive values, and have oxygen species as oxygen. When examining the structure of oxygen-absorbed nanotube structure for the two metals, it can be seen that oxygen is not bonded to the metal atoms.

Since Ni and Cu have saturated d-orbitals, it is very unlikely for them to transfer electrons to oxygen, leading to a less negative bader charge. Consequently, this leads to a weaker oxygen adsorption and a weaker influence of metals on oxygen, corresponding to the positive adsorption energy and short O-O bond length.

Zn displays a highly positive adsorption energy. This is possibly due to the fact that Zn has a full d-orbital, making it less likely to lose electrons to form bond with oxygen that oxygen adsorption energy is very positive.

3.1.2.4.2 Mn to Fe

There is an increase in adsorption energy negativity from Mn to Fe. The drop in adsorption energy negativity from Mn to Fe is likely due to the fact that Fe has 6 electrons in d-orbitals that losing 1 makes it have a half-filled d-orbital. Therefore, Fe is more likely to lose electrons to oxygen and thus forming bond. This is also consistent with the increase in bader charge from Mn to Fe.

3.1.3 Effect of Transition Metal Type on Methane Activation

3.2.1 Effects of Dimension of Nanotube on Embedded Energy

The embedded energies of Fe in nanotubes of different diameters placed below. There is no significant correlation between the value of the embedded energy and the size of the nanotubes. All values are between -6 eV and -11 eV, with the nanotube with chiral indice of 14 being the most negative at -10.6 eV and 12 being the most positive at -6.2 eV.

Chiral Indices (n, m), n = m	Embbedded Energy (eV)
8	-7.44939
10	-7.16228
12	-6.16385
14	-10.605
16	-7.34778
18	-7.5478
20	-7.40415

Table 1. Embedded Energy of Nanotubes with Different Radii

3.2.2 Effect of Dimension of Nanotube on Oxygen Adsorption

The adsorption energies of O_2 on the different FeN_4 nanotubes are shown below in *Table 2*, along with the O-O bond length, bader charges of the oxygen, and oxygen species.

Chiral Indices (n, m), n = m	Adsorption Energy	O-O Bond	Bader Charge-O (eV)	Oxygen Species
8	/	1.296	-0.4684	Peroxide
10	-0.90856	1.298	-0.487	Peroxide
12	-1.09302	1.295	-0.4275	Peroxide
14	-1.11173	1.298	-0.4907	Peroxide
16	-0.8892	1.298	-0.4854	Peroxide
18	-1.05258	1.295	-0.4482	Peroxide
20	-0.86798	1.299	-0.4892	Peroxide
Graphene Surface	-0.88	1.299	-0.52	Peroxide

Table 2. Effect of Dimension of Nanotube on Oxygen Absorption

All adsorption energies are below -0.8, which means that they are negative and thus it would be reasonable to predict an effective adsorption of oxygen onto all sizes. Similarly, a negative bader charge indicates that the oxygen is able to gain electrons, which also shows their potential in being effective single-atom catalysts. The oxygen adsorption strength displays no visible trend in correlation with the radius of the nanotubes, and a similar result is seen in the

bader charge. In comparison with the flat graphene surface, its bader charge is lower, suggesting a more effective charge transfer in the oxygen of the graphene surface. Though, this does not effect the adsorption energy, as the Ead of the nanotubes are more negative than graphene surface except when the (n,m) are equal to 20. All species of oxygen are peroxides, indicating that the fluctuations in adsorption energy and bader charge do not significantly affect the O-O bond length and oxygen species.

3.2.3 Density of State Analysis of Charge Transfer after Adsorption of O_2

As seen in *Figure 8*, the transfer of charges vary in degree in the s, p, and d orbitals. In the transfer of charges in the d orbitals of Fe after adsorption, the increase of nanotube diameter roughly correlates with a decrease in charge transfer. That is, as the curvature of the nanotube in relative to the MN_4-nanotube structure decreases, charge transfer in the d orbital also decreases.

In the p orbital, there is no obvious trend with the radius of nanotubes and the charge transfer. Changes are mostly concentrated between -0.8 eV to -0.11 eV. Most of the nanotubes had an effective transfer in comparison to the positive gain for graphene surfaces.

In the s orbital, little charges are transfered across all the nanotube dimensions. Most charge transfers are concentrated around 0.00 eV to -0.04 eV.

The trend of curvature and charge transfer does not correlate with the bader charge and adsorption energies as the nanotube dimension with lowest adsorption energy and bader charge (14) did not have the highest net transfer of charges.

In comparison to the nanotubes, the Fe on the graphene surface had an overall positive gain of charges. This follows the trend of decreasing charge transfer as curvature decreases, but it does not correlate to the low bader charge of oxygen in the graphene surface.

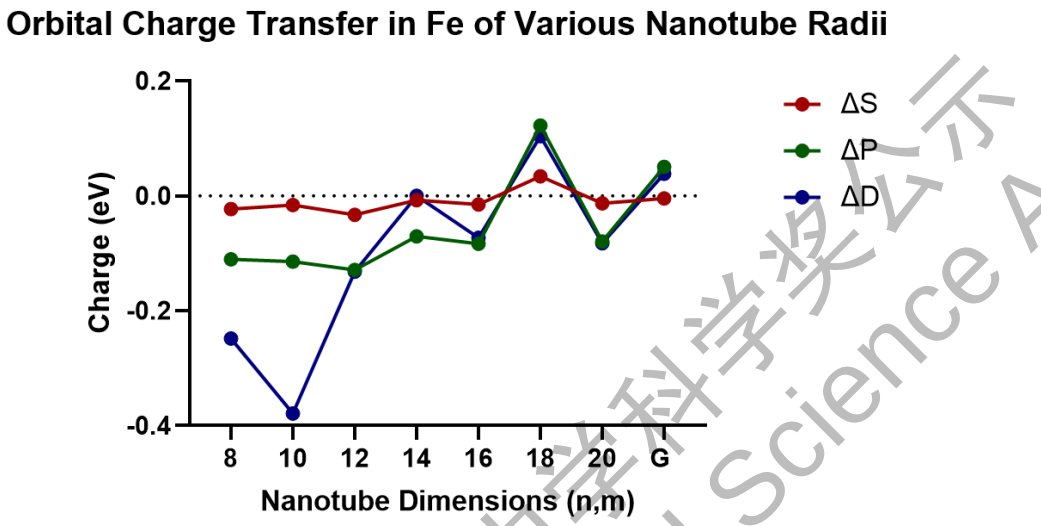

Figure 8. Orbital Charge Transfer in Fe of Various Nanotube Radii

3.2.4 Discussion of Special Points

The nanotube with (n,m)=10 has a higher transfer of charges, it does not correlate with the values of its bader charge and adsorption energy, which was within the range of the different nanotubes.

The nanotube with (n,m)=18 has an unusually high positive charge for the transfer of both s, p, and d orbitals. This means that the central Fe gained charges instead of loosing it to oxygen.

There are no reasonable explanations for these points that could be found yet.

3.2.5 Effect of Radius of Nanotube on Methane Activation

The effect of the nanotube radius on the activation energy of metalloporphyrin oxides activation energy are mostly in between 0.3eV to 0.6eV, shown in *Figure 9* below. This contrasts with the activation energy of methane hydrocarbon bonds in the gaseous state, which is 4.52eV. This shows that both a curved and flat surfaces can effectively reduce the energy barrier of the reaction, increasing the likeliness of a methane hydrocarbon bond activation reaction. The

reduction in energy barrier is most significant in the tubes with indices of 12 and 16, with the lowest one being 0.311 eV. In regards to the graphene surface, there is no significant difference in energy barriers when compared to curved nanotube surfaces.

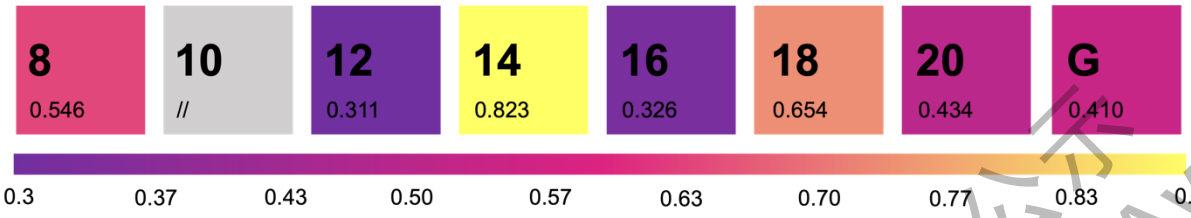

Figure 9. Energy Barrier of Methane Activation in FeN_4 Nanotube of Various Radii

4. Conclusion

Based on previous study, this study provides innovational insights to the use of metal porphyrin oxygen activation as catalyst--the use of nanotubes. Material Studio 8.0 is used to establish molecular structures and VASP is used to optimize structures and calculate embedded energy, adsorption energy, bader charge and activation energy of nanotubes embedded with different period 3 transition metals and that of nanotubes with different radius.

As shown by the results, the adsorption energy and bader charge of nanotubes embedded with different transition metals gradually approaches positive, with O-O bond length gradually decreasing. Among them, nanotubes embedded with Ni, Cu, and Zn display the weakest adsorption of oxygen.

In the investigation on the radii of the nanotubes, the adsorption energies of the various sizes of nanotube tend to be more negative than flat graphene surfaces. The nanotube catalysts are shown to be able to efficively reduce the energy barrier and increase the likeliness of methane hydrocarbon bond activation reactionsTherefore, the main discoveries of this study are:

1. From left to right, transition metals display adsorption approaching to positive values, with all but Ni, Cu, and Zn being negative. Therefore, oxygen adsorption from Sc to Co are all industrially possible. The trend in adsorption energy is likely a result of reducing atomic radius that decreases electrostatic attraction between metals and oxygen.
2. From left to right, transition metals display weaker adsorption energy with lower bader charge. This is likely due to the gradual saturatio of d-orbitals that make rightward transition metals unlikely to lose electrons to oxygen.

3. Apart from Ni, Cu and Zn, the O-O bond length gradually decreases from left to right, signalling a decreasing interaction between metals and oxygen.
4. There are no significant correlation between nanotube radii and catalytic ability, expecially in measurements of adsorption energy and energy barrier change. However, both flat and curved surfaces make effective catalysts for oxygen activation.

References

[1] M. Bradford, M. Vannice, CO2 reforming of CH4, Catal. Rev. 41 (1999) 1-42

[2] X. M. Cao, H. Zhou, L. Zhao, X. Chen, P. Hu, et al. Screening performance of methane activation over atomically dispersed metal catalysts on defective boron nitride monolayers: A density functional theory study. Chinese Chemical Letters 32 (6), 1972-1976.

[3] Allegra A. Latimer, Arvin Kakekhani, Ambarish R. Kulkarni, and Jens K. Nørskov ACS Catalysis 2018 8 (8), 6894-6907 DOI: 10.1021/acscatal.8b00220

[4] Prajapati Aditya, Collins Brianna A, Goodpaster, Jason D. and Singh, Meenesh R. Fundamental insight into electrochemical oxidation of methane towards methanol on transition metal oxides. Proceedings of the National Academy of Sciences. DOI: 10.1073/pnas.2023233118

[5] Priyank Khirsariya, Raju K. Mewada,Single Step Oxidation of Methane to Methanol–Towards Better Understanding,Procedia Engineering,Volume 51, 2013, Pages 409-415, ISSN 1877-7058, https://doi.org/10.1016/j.proeng.2013.01.057.

[6] Vij, V., Tiwari, J., Lee, WG. et al. Hemoglobin-carbon nanotube derived noble-metal-free Fe5C2-based catalyst for highly efficient oxygen reduction reaction. Sci Rep **6**, 20132 (2016). https://doi.org/10.1038/srep20132

[7] A. Krasheninnikov, P. Lehtinen, A. S. Foster, et al., Embedding transition-metal atoms in graphene: structure, bonding, and magnetism, Phy. Rev. Lett. 102 (2009) 126807.

[8] A. Rodríguez-Manzo, O. Cretu, F. Banhart, Trapping of metal atoms in vacancies of carbon nanotubes and graphene, ACS Nano 4 (2010) 3422-3428.

[9] Y. Feng, F. Li, Z. Hu, X. Luo, L. Zhang, X.-F. Zhou, H.-T. Wang, J.-J. Xu, E. Wang, Tuning the catalytic property of nitrogen-doped graphene for cathode oxygen reduction reaction, Phys. Rev. B 85 (2012) 155454.

[10] W. Orellana, Catalytic properties of transition metal–N4 moieties in graphene for the oxygen reduction reaction: evidence of spin-dependent mechanisms, J. Phys. Chem. C 117 (2013) 9812–9818.

[11] Manel Hanana, Hélène Arcostanzo, Pradip K Das, Morgane Bouget, Stéphane Le Gac, et al.. Synergic Effect on Oxygen Reduction Reaction of Strapped Iron Porphyrins Polymerised around Carbon Nanotubes. New Journal of Chemistry, Royal Society of Chemistry, 2018, 42 (24), pp.19749-19754. ff10.1039/C8NJ04516Jff. ffcea-01911991f

[12] C.W. Bezerra, L. Zhang, K. Lee, H. Liu, A.L. Marques, E.P. Marques, H. Wang, J. Zhang, A review of Fe–N/C and Co–N/C catalysts for the oxygen reduction reaction, Electrochim. Acta 53 (2008) 4937–4951.
[13] J. Luque-Centeno, M. Martínez-Huerta, D. Sebastián, G. Lemes, E. Pastor, M. Lázaro, Bifunctional N-doped graphene Ti and Co nanocomposites for the oxygen reduction and evolution reactions, Renew. Energy 125 (2018) 182–192.
[14] Chen X, Hu R, Bai F. DFT Study of the Oxygen Reduction Reaction Activity on Fe-N_4-Patched Carbon Nanotubes: The Influence of the Diameter and Length. Materials (Basel). 2017 May 18;10(5):549. doi: 10.3390/ma10050549. PMID: 28772903; PMCID: PMC5458981.
[15] G. Kresse, J. Furthmuller, Comp. Mater. Sci. 6 (1996) 15-50.
[16] G. Kresse, J. Hafner, Phys. Rev. B 49 (1994) 14251.
[17] G. Kresse, J. Furthmuller, Phys. Rev. B 54 (1996) 11169-11186
[18] J.P. Perdew, K. Burke, M. Ernzerhof, Phys. Rev. Lett. 77 (1996) 3865-3868.
[19] A. Alavi, P. Hu, T. Deutsch, P.L. Silvestrelli, J. Hutter, Phys. Rev. Lett. 80 (1998) 3650-3653
[20] R. Marchiori, 8 - Mathematical Fundamentals of Nanotechnology, Editor(s): Alessandra L. Da Róz, Marystela Ferreira, Fábio de Lima Leite, Osvaldo N. Oliveira, Nanostructures, William Andrew Publishing, 2017, Pages 209-232, ISBN 9780323497824, https://doi.org/10.1016/B978-0-323-49782-4.00008-5.
[21] Qin LC. Determination of the chiral indices (n,m) of carbon nanotubes by electron diffraction. Phys Chem Chem Phys. 2007 Jan 7;9(1):31-48. doi: 10.1039/b614121h. Epub 2006 Nov 22. PMID: 17164886.
[22] Yu, Min; Trinkle, Dallas R. (2011). Accurate and efficient algorithm for Bader charge integration. The Journal of Chemical Physics, 134(6), 064111–. doi:10.1063/1.3553716
[23] Nematollahi, E. C. Neyts, Direct methane conversion to methanol on M and MN4 embedded graphene (M = Ni and Si): A comparative DFT study, Appliced Surface Science 496 (2019) 143618
[24] G. Xu, R. Wang, F. Yang, D. Ma, Z. Yang, Z. Lu, CO oxidation on single Pd atom embedded defect-graphene via a new termolecular Eley-Rideal mechanism, Carbon 118 (2017) 35–42

Appendix

	a (Å)	**b (Å)**	**c (Å)**
8_8	25	25	17.21659
8_8*	18	25	17.21659
10_10*	18	25	17.21659
12_12*	17	25	17.21659
14_14*	25	14	17.21659
16_16*	15	30	17.21659
18_18*	30	18	17.21659
20_20*	35	15	17.21659

*indicates a cleaved nanotube.

Table 3. Dimensions of Periodic Slabs

Acknowledgements

Out of the interest to further explore the field of chemistry, we have devoted efforts into learning deeper chemistry knowledge. Under the guidance of Ms. Jialong Liu and Professor Xiaoming Cao, we encountered a novel field of chemistry--computational chemistry. Following their guidance, we learnt calculation methods in computational chemistry with multiple softwares.

With a primary understanding of the field of computational chemistry, we read research papers in this field to form a more thorough understanding of its application. In the process of learning, we have encountered the concept of catalyst, which we learnt is crucial to our lives. To form more understandings about this topic, we read research papers and learnt the use of poriphrin in catalysis, discovering the unique cylindrical structure of nanotube that can potentially be applied.

To understand the possiblity of using nanotubes for oxygen activation, we decided to conduct a scientific research about this topic through computational chemistry techniques. During the process of experimental design, Ms. Jialong Liu provided constructive suggestions in the possible directions to reach for. During the process of calculation, Ms. Jialong Liu and Professor Xiaoming Cao provided technical support and inspired us in understanding of calculated data.

During the process of calculation, works are distributed equally between the team, with Tianjia Cheng calculating data for nanotubes embedded with different transition metals, and Adeline Hung calculating data for nanotubes of different radii.

Through the process of conducting scientific research, we are able to explore a novel field of chemistry, to enhance our understanding of chemistry, and to provide insights to the real-world problem of catalysis.